Desalination and Water Treatment
www.deswater.com

doi: 10.1080/19443994.2013.827818

52 (2014) 6712–6719
October

Taylor & Francis
Taylor & Francis Group

Adsorption of methylene blue onto papaya leaves: comparison of linear and nonlinear isotherm analysis

R.R. Krishni[a], K.Y. Foo[b], B.H. Hameed[a,*]

[a]*School of Chemical Engineering, Engineering Campus, Universiti Sains Malaysia, Nibong Tebal, Penang 14300, Malaysia*
Tel. +604-5996422; Fax: +604-5941013; email: chbassim@eng.usm.my
[b]*Environment and Occupational Health Programme, School of Health Sciences, Health Campus, Universiti Sains Malaysia, Kubang Kerian, Kelantan 16150, Malaysia*

Received 2 August 2012; Accepted 26 June 2013

ABSTRACT

The use of low-cost adsorbent papaya leaf was investigated as a replacement for current costly methods of removing methylene blue dye (MB) from the aqueous solution. The adsorption equilibrium was determined as a function of contact time, initial adsorbate concentration, and solution pH. The adsorptive uptake of MB increased with increasing the initial MB concentration and solution pH. The adsorption isotherms were correlated with a comparison of linear and nonlinear regression analysis. Langmuir isotherm model provided the best-fit for the adsorption of MB onto papaya leaf, with a maximum monolayer adsorption capacity of 231.65 mg/g. This locally available adsorbent was found to be low cost and promising for the remediation of textile wastewater.

Keywords: Adsorption; Equilibrium; Isotherm; Kinetic; Methylene blue; Papaya leaf

1. Introduction

Papaya (*Carica papaya*) is a tropical plant species within the family Caricaceae, widely cultivated for the consumption of fresh fruit, drinks, jam candies and crystallized fruit [1]. Papaya tree is a soft-wooded perennial plant, with the cylindrical trunk of 30 cm in diameter, and growing 8–10 m in height. Biochemically, papaya fruit is an excellent source of calcium, vitamin A, vitamin C, and several proteins and alkaloids, with important pharmaceutical and industrial applications [2]. The black seeds are grounded as a substitute for black pepper [3]. However, the papaya leaves which have low economic values are usually discarded as waste. A promising option is converting them into a renewable and low-cost adsorbent.

Adsorption process, a surface phenomenon by which a multi-components fluid mixture is attracted to the surface of solid adsorbents and form attachments via physical or chemical bonds, is recognized as the most efficient fundamental approach in wastewater treatment processes [4]. In the endeavor to develop an adsorption system, it is essential to establish the most appropriate correlation, which is indispensable for reliable prediction of adsorption parameters and quantitative comparison of adsorbent behavior for different adsorbate–adsorbent systems [5].

Adsorption isotherm is an invaluable tool describing the mobility of adsorbate substance from aqueous

*Corresponding author.

media to the solid-phase adsorbents [6]. These equilibrium models provide an insight into the adsorption mechanism and surface properties of the adsorbent [7]. Linear regression is the most widely used technique to estimate the adsorption isotherm parameters [8]. However, recent studies have demonstrated that the linearization of the isotherm expressions may alter the error distribution, resulting in different outcomes [9,10]. This study was conducted to examine the potential of papaya leaf as a renewable low-cost adsorbent for removing methylene blue dye (MB) from the aqueous solutions. The morphological structure and surface chemistry of the prepared adsorbent were investigated. The effect of initial dye concentration, contact time, and solution pH on the adsorptive uptake of MB is evaluated. Moreover, a comparison between the linear and nonlinear analysis for estimating the isotherm parameters was outlined.

2. Materials and methods

2.1. Adsorbate

MB, a cationic pollutant difficult to be degraded in natural environment, was selected as the model adsorbate in this study. The standard stock solution was prepared by dissolving accurately weight dye in double distilled water to a concentration of 1,000 mg/L. The working solutions were prepared by successive dilution.

2.2. Preparation and characterization of adsorbent

Papaya leaves, lignocellulosic biomass abundantly available in the papaya plantation area, were chosen as the raw material in this work. The material was cut into small pieces, washed repeatedly with hot distilled water, air-dried, crushed, and sieved to a geometrical mean size of 500 μm. The surface morphology was examined using the scanning electron microscopy (SEM), while the surface functional groups were detected by Fourier transform infrared (FTIR) spectroscope (FTIR-2000, Perkin–Elmer) from the scanning range of 4,000–400 cm^{-1}.

2.3. Batch equilibrium studies

The batch adsorption studies were undertaken using a set of Erlenmeyer flasks (250 mL) containing 0.30 g of adsorbent and 200 mL of MB solutions at the concentrations of 50–300 mg/L. The flasks were placed in an isothermal water bath shaker at 30˚C till the equilibrium. The concentrations of MB were determined using a UV–vis spectrophotometer (Shimadzu UV/vis 1601 spectrophotometer, Japan) at the maximum wavelength of 668 nm. The MB uptake at time t, q_t (mg/g) and equilibrium, q_e (mg/g), was calculated by:

$$q_t = \frac{(C_0 - C_t)V}{W} \quad (1)$$

$$q_e = \frac{(C_0 - C_e)V}{W} \quad (2)$$

where C_0, C_t, and C_e (mg/L) are the liquid-phase concentrations of dye at initial, time t (min) and equilibrium, respectively. V is the volume of the solution (L), and W is the mass of adsorbent used (g). The effect of initial pH on the adsorptive uptake of MB adsorption was carried out by adjusting the pH in the range of 2–10, at the fixed MB concentration of 200 mg/L, adsorbent dosage of 0.3 g/200 mL, and adsorption temperature of 30˚C. The pH was measured using a pH meter (Model Delta 320, Mettler Toledo, China).

2.4. Adsorption isotherm

2.4.1. Langmuir isotherm model

Langmuir adsorption isotherm [11] is an empirical model describing monolayer adsorption, with no lateral interaction and steric hindrance between the adsorbed molecules, even on the adjacent sites:

$$q_e = \frac{Q_0 K_L C_e}{1 + K_L C_e} \quad (3)$$

where Q_0 (mg/g) and K_L (L/g) are Langmuir constants related to adsorption capacity and rate of adsorption.

2.4.2. Freundlich isotherm model

Freundlich isotherm [12] refers to the non-ideal and reversible adsorption, with non-uniform distribution of adsorption heat and affinities over the heterogeneous surface:

$$q_e = K_F C_e^{1/n} \quad (4)$$

where K_F (mg/g).(L/mg)$^{1/n}$ and $1/n$ are the Freundlich adsorption constant and a measure of adsorption intensity.

2.4.3. Temkin isotherm model

Temkin isotherm [13] assumes the heat of adsorption of all molecules in the layer would decrease linearly rather than logarithmically with surface coverage:

$$q_e = B \ln(AC_e) \quad (5)$$

where $B = RT/b$, and b (J/mol), A (L/g), R (8.314 J/mol K), and T (K) are the Temkin constant related to heat of sorption, equilibrium binding constant, gas constant, and absolute temperature.

3. Results and discussion

3.1. Characterization of the prepared adsorbent

The surface morphology of the papaya leaves before and after the adsorption of MB was visualized via SEM as shown in Fig. 1. Examination of SEM micrographs identified the presence of high pores structure over the surface of papaya leaves (Fig. 1(a)). However, the surface of the dye-loaded adsorbent displayed a rougher texture covered with the adsorbed dye molecules (Fig. 1(b)). Comparison of these micrographs before and after the sorption of MB illustrated the adsorption of MB over the surface of papaya leaves.

The obtained FTIR spectrum of papaya leaves (Table 1) reveals major peaks at 3,345/3,338, 2,919/2,918, 2,850, 1,733, 1,627/1,626, 1,445/1,442, 1,393, 1,377, 1,355, 1,318/1,317, 1,257-1,203, 1,157/1,148, 1,061/1,053, 1,037, 893–830, 781/780, and 669/667 cm^{-1}, identical to the presence of –OH, $–CH_2$, CH, C=O, C=C, CH_2 deformation, H–C=O aliphatic aldehydes, CH_3 deformation, NO_2 aromatic compounds,

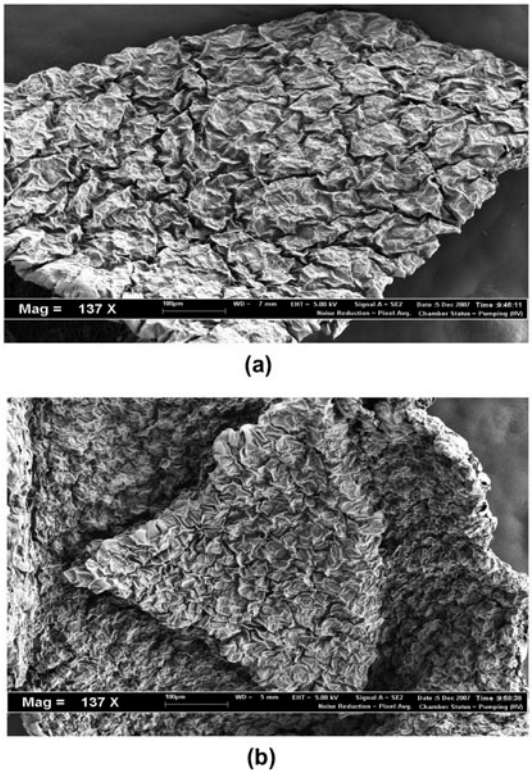

Fig. 1. SEM micrographs for the papaya leaves derived adsorbent (a) before and (b) after the adsorption of MB (137 X).

Table 1
Comparison FTIR spectroscopy of the papaya leaves derived adsorbent before and after the adsorption of MB

IR peak	Frequency (cm^{-1})		Assignation
	Before adsorption	After adsorption	
1	3,345	3,338	Bonded –OH groups
2	2,919	2,918	Two bands for $–CH_2$-groups
3	2,850	–	CH stretch
4	1,733	–	C = O stretch
5	1,627	1,626	C = C stretch
6	1,445	1,442	CH_2 deformation
7	–	1,393	H–C = O bends aliphatic aldehydes
8	1,377	–	CH_3 deformation
9	–	1,355	$–NO_2$ aromatic nitro compounds
10	1,317	1,318	C–O–H bend
11	1,257–1,203	1,249	C–O–C stretch
12	1,157	1,148	C–N stretch
13	1,053	1,061	S = O alkyl sulfoxides
14	–	1,037	P–O–C strongest band highest frequencies for aliphatic amines
15	893	886–830	CH out-of-plane deformation
16	780	781	C–Cl stretch
17	669	667	C–O–H twist broad

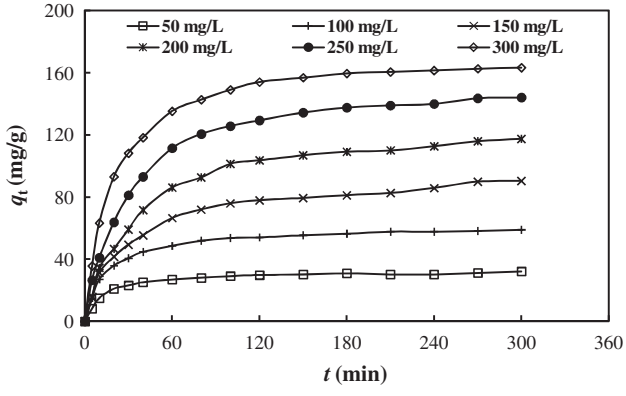

Fig. 2. Effect of initial concentration and contact time on the adsorptive uptake of MB onto the papaya leaves derived adsorbent (conditions: $W = 0.30$ g/200 mL; temperature = 30°C).

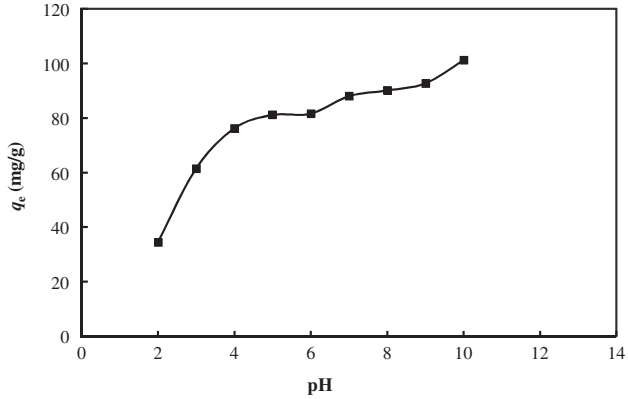

Fig. 3. Effect of solution pH on the adsorption of MB onto the papaya leaves derived adsorbent (conditions: $W = 0.30\,g/200\,mL$; $C_0 = 200\,mg/L$; temperature 30°C).

C–O–H, C–O–C, C–N, alkyl S=O sulfoxides, P–O–C, out-of-plane CH deformation, C–Cl, and twist C–O–H derivatives. The surface chemistry of the papaya leaves derived adsorbent detected some shift, disappear and new peaks after the sorption of MB, indicating possible involvement of the functional groups during the adsorption process.

3.2. Batch adsorption studies

The curve adsorption uptake of MB, q_t as a function of time, t at the initial concentrations 50–300 mg/L is displayed in Fig. 2. The adsorption capacity increased with prolonging the contact time. It is clear from Fig. 2 that the adsorption process increased sharply at the initial stage, indicating the availability of readily accessible sites. The process is gradually slower as the equilibrium approached. The time required to attain this state of equilibrium is termed as equilibrium time [14]. In the present study, the adsorption equilibrium, q_e, increased from 32.11 to 163.30 mg/g with an increase in initial concentration from 50 to 300 mg/L, mainly ascribed to the higher concentration gradient which acts as a driving force for the adsorption process [15].

The effect of pH was conducted by varying the pH of dye solutions from 2 to 10, with an initial concentration of 200 mg/L, as shown in Fig. 3. Increase in solution pH exerted an enhancement of adsorptive uptake of MB from 34.46 to 101.20 mg/g, mainly associated with the protonation of MB in the acidic medium, and high mobility of H_3O^+ ions competing with dye cations for the adsorption surface. At higher solution pH, the papaya leaf derived adsorbent may get negatively charged and the formation of electric double layer changes its polarity, consequently the dye uptake increases [16].

3.3. Adsorption isotherm

Adsorption isotherms are essential to the practical design and optimization of the adsorption systems [17]. In the present work, a comparison between the linear and nonlinear Langmuir, Freundlich, and

Table 2
Linear and nonlinear form of Langmuir, Freundlich, and Temkin isotherm models

Isotherm	Nonlinear form	Linear form	Plot	Reference
Langmuir-1	$q_e = \frac{Q_0 b C_e}{1 + b C_e}$	$\frac{C_e}{q_e} = \frac{1}{bQ_0} + \frac{C_e}{Q_0}$	$\frac{C_e}{q_e}$ vs. C_e	[11]
Langmuir-2		$\frac{1}{q_e} = \frac{1}{Q_0} + \frac{1}{bQ_0 C_e}$	$\frac{1}{q_e}$ vs. $\frac{1}{C_e}$	
Langmuir-3		$q_e = Q_0 - \frac{q_e}{bC_e}$	q_e vs. $\frac{q_e}{C_e}$	
Langmuir-4		$\frac{q_e}{C_e} = bQ_0 - bq_e$	$\frac{q_e}{C_e}$ vs. q_e	
Freundlich	$q_e = K_F C_e^{\frac{1}{n}}$	$\log q_e = \log K_F + \frac{1}{n} \log C_e$	$\log q_e$ vs. $\log C_e$	[12]
Temkin	$q_e = \frac{RT}{b_T} \ln A_T C_e$	$q_e = \frac{RT}{b_T} \ln A_T + \left(\frac{RT}{b_T}\right) \ln C_e$	q_e vs. $\ln C_e$	[13]

Temkin isotherm was established (Table 2). The applicability of the isotherm equation was judged by determination of coefficient of determination, R^2.

$$R^2 = \frac{\sum(q_{cal} - q_{m,exp})^2}{\sum(q_{cal} - q_{m,exp})^2 + \sum(q_{cal} - q_{exp})^2} \quad (6)$$

where q_{exp} (mg/g) is the equilibrium uptake of MB experimentally, q_{cal} is the equilibrium uptake of MB theoretically, and $q_{m,exp}$ is the average q_{exp} (mg/g).

For linear regression analysis, the Langmuir isotherm constants related to adsorption capacity, Q_0 (mg/g) and rate of adsorption, K_L (dm^3/g) for Langmuir-1, Langmuir-2, Langmuir-3, and Langmuir-4 were predicted from the plots between C_e/q_e vs. C_e, $1/q_e$ vs. $1/C_e$, q_e vs. q_e/C_e, and q_e/C_e vs. q_e, respectively. Similarly, the Freundlich isotherm constants, K_F (mg/g) (L/mg)^n and $1/n$, can be calculated from the plot of log (q_e) vs. log (C_e), while Temkin isotherm constants, B and A (L/g) were determined from the linear curve of q_e vs. 1n (C_e).

For nonlinear regression, a trial and error procedure, which is applicable to computer operation, was developed to determine the isotherm parameters by maximizing the respective coefficient of determination between experimental data and the isotherms. Figs. 4–6 show the experimental data and the predicted equilibrium curve for the three-equilibrium isotherm at 333 K. The obtained isotherm constants for the three isotherm models and their corresponding R^2 are listed in Table 3. It was observed that the Langmuir isotherm constants varied for different forms of linear Langmuir equations. The different outcomes shown by the four linearized forms of Langmuir isotherm models indicate mathematical complexities associated with linear method in estimating the rate parameters. The difference between the predicted and experimental equilibrium data by different linear expressions can be due to the prob-

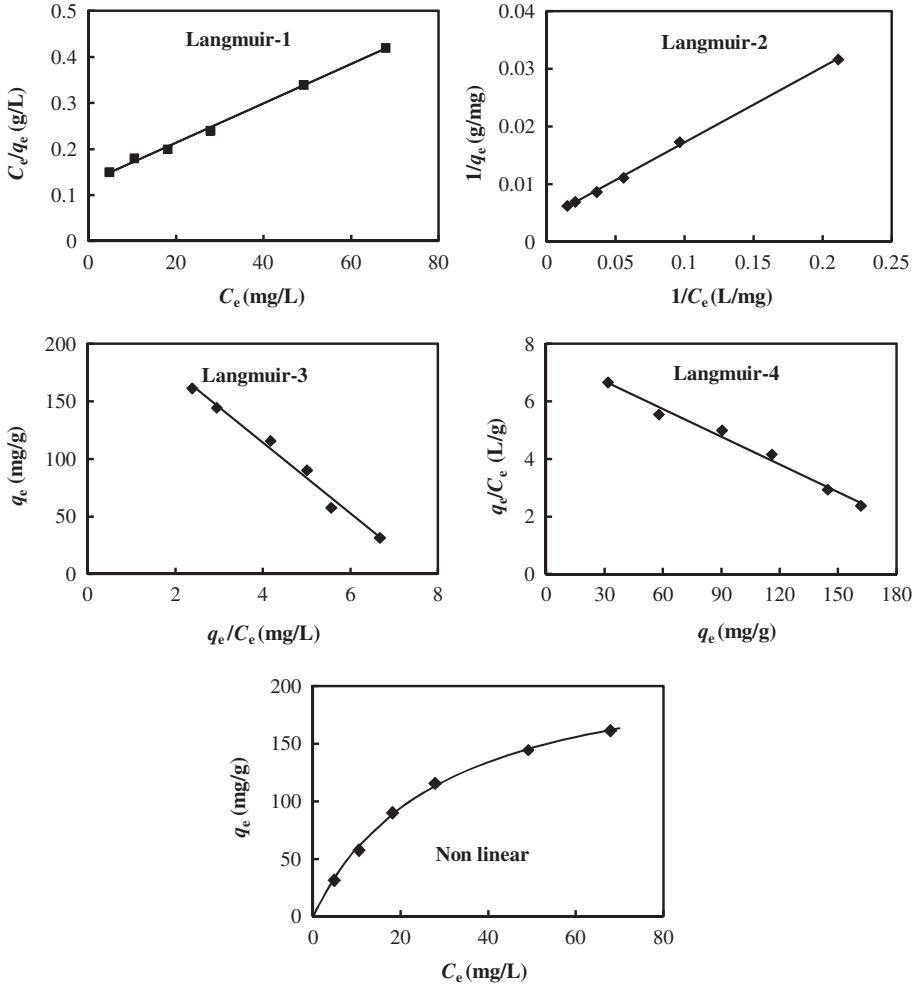

Fig. 4. Plot of Langmuir isotherm models for the adsorption of MB onto papaya leaves derived adsorbent at 30°C.

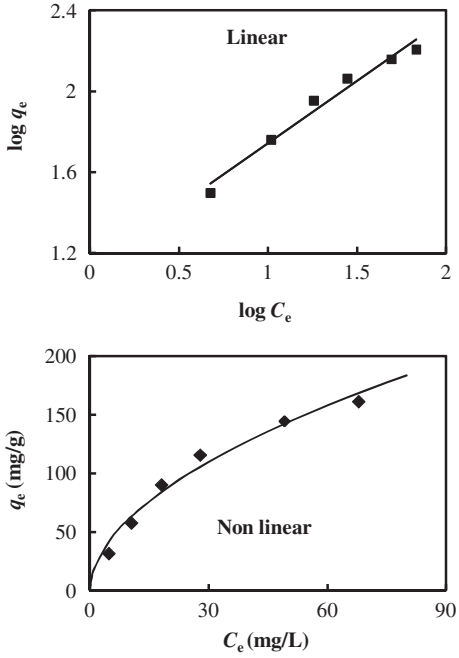

Fig. 5. Plots of Freundlich isotherm models for the adsorption of MB onto papaya leaves derived adsorbent at 30°C.

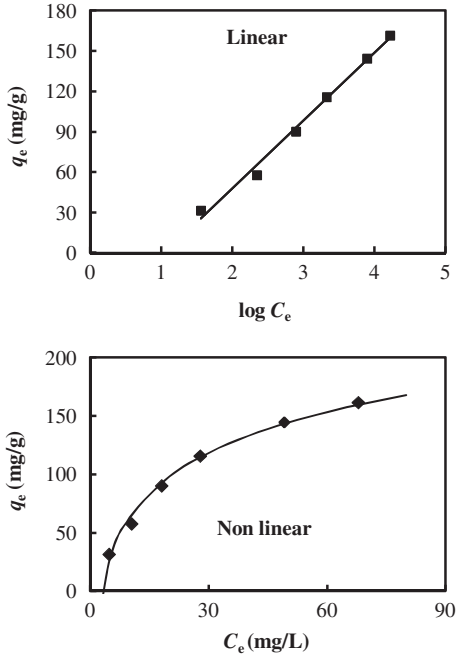

Fig. 6. Plots of Temkin isotherm models for the adsorption of MB onto papaya leaves derived adsorbent at 30°C.

lems with transformation of nonlinear to linear expression which will distort the experimental error and the normality assumptions of least squares method [18]. Besides, the linear method assumes that the scatter of points around the line follows a Gaussian distribution and the error distribution is same at every value of X, but this is practically impossible as the error distribution may get altered after transformed to a linear form [19].

However, there are no problems with nonlinear Langmuir isotherm equation as they are in the same error structures. When comparing R^2 values of the isotherm models, the theoretical assumption of Langmuir isotherm model was getting valid for Langmuir-2 and non-Langmuir isotherm models, while Freundlich and Temkin isotherms did not much well represent the adsorption data. The result suggests that the adsorption takes place on homogeneous sites that are identical and energetically equivalent. The findings also demonstrate no interaction and transmigration of dyes in the plane of the neighboring surface [20]. Table 4 summarizes a comparative evaluation of the adsorption capacities for MB onto different

Table 3
Isotherm parameters obtained by linear and nonlinear Langmuir, Freundlich, and Temkin isotherm models for the adsorption of MB onto papaya leaves derived adsorbent

Isotherm	Isotherm constants	
Langmuir-1	Q_0 (mg/g)	233.95
	K_L (L/mg)	0.033
	R^2	0.996
Langmuir-2	Q_0 (mg/g)	239.57
	K_L (L/mg)	0.032
	R^2	0.998
Langmuir-3	Q_0 (mg/g)	237.30
	K_L (L/mg)	0.032
	R^2	0.982
Langmuir-4	Q_0 (mg/g)	239.25
	K_L (L/mg)	0.030
	R^2	0.982
Nonlinear Langmuir	Q_0 (mg/g)	231.65
	K_L (L/mg)	0.034
	R^2	0.998
Linear Freundlich	K_F (mg/g) (L/mg)$^{1/n}$	13.42
	n	1.62
	R^2	0.967
Nonlinear Freundlich	K_F (mg/g) (L/mg)$^{1/n}$	18.48
	n	1.91
	R^2	0.974
Linear Temkin	A (L/g)	0.34
	B	50.31
	R^2	0.989
Nonlinear Temkin	A (L/g)	0.36
	B	50.40
	R^2	0.992

Table 4
Comparison of adsorption capacities of MB onto different adsorbents

Adsorbent	Q_0 (mg/g)	References
Papaya leave	231.60	This study
Cottonseed hull	185.22	[21]
Natural zeolite	19.94	[22]
Natural palygorskite clay	48.39	[23]
Fly ash	10.20	[24]
Graphene	153.85	[25]
Date stone activated carbon	316.11	[26]
Pistachio nut shell activated carbon	296.57	[27]
Palm fiber activated carbon	312.50	[28]

adsorbents. The adsorbent prepared in this work showed relatively high adsorption capacity for MB of 231.65 mg/g, as compared to some previous works [21–28] as reported in the literature.

4. Conclusion

The study indicated the suitability of papaya leaves for removing MB from the aqueous solution. Increases in MB concentration, contact time, and solution pH were found to increase the adsorptive uptake of MB. Adsorption isotherm showed that Langmuir isotherm model fits well with the experimental data. The nonlinear regression method provided a better estimation for the adsorption of MB onto papaya leaves, suggesting a monolayer adsorption capacity of 231.65 mg/g. The adsorbent could be employed to treat MB enriched wastewater.

References

[1] D. Gonsalves, Control of papaya ringspot virus in papaya: A case study, Annu. Rev. Phytopathol. 36 (1998) 415–437.
[2] J. Morton, Papaya, in: J.F. Morton (Ed.), Fruits of Warm Climates, Creative Resource Systems, Miami, FL, 1987, pp. 336–346.
[3] N.K. Lohiya, B. Manivannan, P.K. Mishra, N. Pathak, S. Sriram, S.S. Bhande, S. Panneerdoss, Chloroform extract of *Carica papaya* seeds induces long-term reversible azoospermia in langur monkey, Asian J. Andrology 4 (2002) 17–26.
[4] K.Y. Foo, B.H. Hameed, Potential of activated carbon adsorption processes for the remediation of nuclear effluents: A recent literature, Desalin. Water Treat. 41 (2012) 72–78.
[5] K.Y. Foo, B.H. Hameed, Adsorption characteristics of industrial solid waste derived activated carbon prepared by microwave heating for methylene blue, Fuel Process. Technol. 99 (2012) 103–109.
[6] K.Y. Foo, B.H. Hameed, Microwave-assisted preparation and adsorption performance of activated carbon from biodiesel industry solid reside: Influence of operational parameters, Bioresour. Technol. 103 (2012) 398–404.
[7] K.Y. Foo, B.H. Hameed, Preparation and characterization of activated carbon from melon seed oil (Citrullus vulgaris) residue via microwave induced NaOH activation, Desalin. Water Treat. 47 (2012) 130–138.
[8] M.A. Abdullah, L. Chiang, M. Nadeem, Comparative evaluation of adsorption kinetics and isotherms of a natural product removal by amberlite polymeric adsorbents, Chem. Eng. J. 146 (2009) 370–376.
[9] K.Y. Foo, B.H. Hameed, Microwave assisted preparation of activated carbon from pomelo skin for the removal of anionic and cationic dyes, Chem. Eng. J. 173 (2011) 385–390.
[10] K.Y. Foo, B.H. Hameed, Insights into the modeling of adsorption isotherm systems, Chem. Eng. J. 156 (2010) 2–10.
[11] I. Langmuir, The adsorption of gases on plane surfaces of glass, mica and platinum, J. Am. Chem. 57 (1918) 1361–1403.
[12] H. Freundlich, Über die adsorption in lösungen (adsorption in solution), Z. Phys. Chem. 57 (1906) 384–470.
[13] M.I. Tempkin, V. Pyzhev, Kinetics of ammonia synthesis on promoted iron catalyst, Acta Phys. Chim. USSR 12 (1940) 327–356.
[14] Y.L. Liu, D. Ma, J.L. Li, X.R. Zhao, R.P. Han, Characterization of bio-char from pyrolysis of wheat straw and its evaluation on methylene blue adsorption, Desalin. Water Treat. 46 (2012) 115–123.
[15] V. Mishra, C. Balomajumde, V.K. Agarwal, Sorption of Zn(II) ion onto the surface of activated carbon derived from eucalyptus bark saw dust from industrial wastewater: Isotherm, kinetics, mechanistic modeling, and thermodynamics, Desalin. Water Treat. 46 (2012) 332–351.
[16] O. Kerkez, S.S. Bayazit, H. Uslu, A comperative study for adsorption of methylene blue from aqueous solutions by two kinds of amberlite resin materials, Desalin. Water Treat. 45 (2012) 206–214.
[17] K.Y. Foo, L.K. Lee, B.H. Hameed, Preparation of activated carbon from sugarcane bagasse by microwave assisted activation for the remediation of semi-aerobic landfill leachate, Bioresour. Technol. 134 (2013) 166–172.
[18] K.V. Kumar, K. Porkodi, F. Rocha, Comparison of various error functions in predicting the optimum isotherm by linear and non-linear regression analysis for the sorption of basic red 9 by activated carbon, J. Hazard. Mater. 150 (2008) 158–165.
[19] D. Kalderis, D. Koutoulakis, P. Paraskeva, E. Diamadopoulos, E. Otal, J.O. del Valle, C.F. Pereira, Adsorption of polluting substances on activated carbons prepared from rice husk and sugarcane bagasse, Chem. Eng. J. 144 (2008) 42–50.
[20] B. Boulinguiez, P.L. Cloirec, D. Wolbert, Revisiting the determination of Langmuir parameters application to tetrahydrothiophene adsorption onto activated carbon, Langmuir 24 (2008) 6420–6424.
[21] Q. Zhou, W.Q. Gong, C.X. Xie, Y.B. Li, C.P. Bai, S.H. Chen, Biosorption of methylene blue from aqueous solution on spent cottonseed hull substrate for Pleurotus ostreatus cultivation, Desalin. Water Treat. 29 (2011) 317–325.
[22] R.P. Han, J.J. Zhang, P. Han, Y.F. Wang, Z.H. Zhao, M.S. Tang, Study of equilibrium, kinetic and thermodynamic parameters about methylene blue adsorption onto natural zeolite, Chem. Eng. J. 145 (2009) 496–504.
[23] H. Chen, J. Zhao, A.G. Zhong, Y.X. Jin, Removal capacity and adsorption mechanism of heat-treated palygorskite clay for methylene blue, Chem. Eng. J. 174 (2011) 143–150.
[24] Q. Liu, Y.M. Zhou, L.Q. Zou, T. Deng, J. Zhang, Y. Sun, X.X. Ruan, P. Zhu, G.R. Qian, Simultaneous wastewater decoloration and fly ash dechlorination during the dye wastewater treatment by municipal solid waste incineration fly ash, Desalin. Water Treat. 32 (2011) 179–186.
[25] T. Liu, Y. Li, Q. Du, J. Sun, Y. Jiao, G. Yang, Z. Wang, Y. Xia, W. Zhang, K. Wang, H. Zhu, D. Wu, Adsorption of methylene blue from aqueous solution by grapheme, Colloids Surf. B 90 (2012) 197–203.
[26] K.Y. Foo, B.H. Hameed, Preparation of activated carbon from date stones by microwave induced chemical activation: Application for methylene blue adsorption, Chem. Eng. J. 170 (2011) 338–341.

[27] K.Y. Foo, B.H. Hameed, Preparation and characterization of activated carbon from pistachio nut shells via microwave-induced chemical activation, Biomass Bioenergy 35 (2011) 3257–3261.

[28] K.Y. Foo, B.H. Hameed, Microwave-assisted preparation of oil palm fiber activated carbon for methylene blue adsorption, Chem. Eng. J. 166 (2011) 792–795.